

3. Klinman, D. M. Immunotherapeutic uses of CpG oligodeoxynucleotides. *Nature Rev. Immunol.* **4**, 249–258 (2004).
4. Krieg, A. M. CpG motifs in bacterial DNA and their immune effects. *Annu. Rev. Immunol.* **20**, 709–760 (2002).
5. Theofilopoulos, A. N., Baccala, R., Beutler, B. & Kono, D. H. Type I interferons ( $\alpha/\beta$ ) in immunity and autoimmunity. *Annu. Rev. Immunol.* **23**, 307–335 (2005).
6. Ronnblom, L. & Alm, G. V. Systemic lupus erythematosus and the type I interferon system. *Arthritis Res. Ther.* **5**, 68–75 (2003).
7. Honda, K. *et al.* IRF-7 is the master regulator of type-I interferon-dependent immune responses. *Nature* advance online publication, 30 March 2005 (doi:10.1038/nature03464).
8. Verthelyi, D., Ishii, K. J., Gursel, M., Takeshita, F. & Klinman, D. M. Human peripheral blood cells differentially recognize and respond to two distinct CpG motifs. *J. Immunol.* **166**, 2372–2377 (2001).
9. Krug, A. *et al.* Identification of CpG oligonucleotide sequences with high induction of IFN- $\alpha/\beta$  in plasmacytoid dendritic cells. *Eur. J. Immunol.* **31**, 2154–2163 (2001).
10. Hemmi, H., Kaisho, T., Takeda, K. & Akira, S. The roles of Toll-like receptor 9, MyD88, and DNA-dependent protein kinase catalytic subunit in the effects of two distinct CpG DNAs on dendritic cell subsets. *J. Immunol.* **170**, 3059–3064 (2003).
11. Kerkmann, M. *et al.* Activation with CpG-A and CpG-B oligonucleotides reveals two distinct regulatory pathways of type I IFN synthesis in human plasmacytoid dendritic cells. *J. Immunol.* **170**, 4465–4474 (2003).
12. Krieg, A. M. *et al.* CpG motifs in bacterial DNA trigger direct B-cell activation. *Nature* **374**, 546–549 (1995).
13. Izaguirre, A. *et al.* Comparative analysis of IRF and IFN- $\alpha$  expression in human plasmacytoid and monocyte-derived dendritic cells. *J. Leukoc. Biol.* **74**, 1125–1138 (2003).
14. Coccia, E. M. *et al.* Viral infection and Toll-like receptor agonists induce a differential expression of type I and  $\lambda$  interferons in human plasmacytoid and monocyte-derived dendritic cells. *Eur. J. Immunol.* **34**, 796–805 (2004).
15. Latz, E. *et al.* TLR9 signals after translocating from the ER to CpG DNA in the lysosome. *Nature Immunol.* **5**, 190–198 (2004).
16. Honda, K. *et al.* Role of a transductional-transcriptional processor complex involving MyD88 and IRF-7 in Toll-like receptor signaling. *Proc. Natl Acad. Sci. USA* **101**, 15416–15421 (2004).
17. Takaoka, A. *et al.* Integral role of IRF-5 in the gene induction programme activated by Toll-like receptors. *Nature* **434**, 243–249 (2005).
18. Zabner, J., Fasbender, A. J., Moninger, T., Poellinger, K. A. & Welsh, M. J. Cellular and molecular barriers to gene transfer by a cationic lipid. *J. Biol. Chem.* **270**, 18997–19007 (1995).
19. Heil, F. *et al.* Species-specific recognition of single-stranded RNA via toll-like receptor 7 and 8. *Science* **303**, 1526–1529 (2004).
20. Diebold, S. S., Kaisho, T., Hemmi, H., Akira, S. & Reis e Sousa, C. Innate antiviral responses by means of TLR7-mediated recognition of single-stranded RNA. *Science* **303**, 1529–1531 (2004).
21. Heil, F. *et al.* The Toll-like receptor 7 (TLR7)-specific stimulus loxoribine uncovers a strong relationship within the TLR7, 8 and 9 subfamily. *Eur. J. Immunol.* **33**, 2987–2997 (2003).
22. Hacker, H. *et al.* CpG-DNA-specific activation of antigen-presenting cells requires stress kinase activity and is preceded by non-specific endocytosis and endosomal maturation. *EMBO J.* **17**, 6230–6240 (1998).
23. Hacker, H. *et al.* Immune cell activation by bacterial CpG-DNA through myeloid differentiation marker 88 and tumor necrosis factor receptor-associated factor (TRAF)6. *J. Exp. Med.* **192**, 595–600 (2000).
24. Radler, J. O., Koltover, I., Salditt, T. & Safinya, C. R. Structure of DNA-cationic liposome complexes: DNA intercalation in multilamellar membranes in distinct interhelical packing regimes. *Science* **275**, 810–814 (1997).
25. Koltover, I., Salditt, T., Radler, J. O. & Safinya, C. R. An inverted hexagonal phase of cationic liposome–DNA complexes related to DNA release and delivery. *Science* **281**, 78–81 (1998).
26. Durrer, P., Gaudin, Y., Ruigrok, R. W., Graf, R. & Brunner, J. Photolabeling identifies a putative fusion domain in the envelope glycoprotein of rabies and vesicular stomatitis viruses. *J. Biol. Chem.* **270**, 17575–17581 (1995).
27. Brunetti, C. R., Dingwell, K. S., Wale, C., Graham, F. L. & Johnson, D. C. Herpes simplex virus gD and virions accumulate in endosomes by mannose 6-phosphate-dependent and -independent mechanisms. *J. Virol.* **72**, 3330–3339 (1998).
28. Leadbetter, E. A. *et al.* Chromatin–IgG complexes activate B cells by dual engagement of IgM and Toll-like receptors. *Nature* **416**, 603–607 (2002).
29. Mellman, I. Endocytosis and molecular sorting. *Annu. Rev. Cell Dev. Biol.* **12**, 575–625 (1996).
30. Asselin-Paturel, C., Brizard, G., Pin, J. J., Briere, F. & Trinchieri, G. Mouse strain differences in plasmacytoid dendritic cell frequency and function revealed by a novel monoclonal antibody. *J. Immunol.* **171**, 6466–6477 (2003).

**Supplementary Information** accompanies the paper on [www.nature.com/nature](http://www.nature.com/nature).

**Acknowledgements** We thank J. Vilcek, H. Rosen, H. Ohno, F. Nakatsu, A. Nakano, M. Lamphier, L. Cantley and T. Curran for advice, S. Akira for TLR9 and MyD88 mutant mice, G. Trinchieri for the pDC-specific antibody, A. Miyawaki for Venus (a variant of YFP), H. Miyoshi for lentivirus vectors, and M. Shishido for technical assistance. This work was supported in part by a grant for Advanced Research on Cancer and a Grant-In-Aid for Scientific Research on Proprietary Areas from the Ministry of Education, Culture, Sports, Science and Technology of Japan, the Uehara Memorial Foundation, the Sumitomo Foundation, the Senri Life Science Foundation and the Nakajima Foundation. H.N. was supported by an Ishidu Shun Memorial Scholarship.

**Competing interests statement** The authors declare that they have no competing financial interests.

**Correspondence** and requests for materials should be addressed to T.T. ([tada@m.u-tokyo.ac.jp](mailto:tada@m.u-tokyo.ac.jp)).

## Visualizing the mechanical activation of Src

Yingxiao Wang<sup>1</sup>, Elliot L. Botvinick<sup>1,5</sup>, Yihua Zhao<sup>1</sup>, Michael W. Berns<sup>1,4,5</sup>, Shunichi Usami<sup>1</sup>, Roger Y. Tsien<sup>3</sup> & Shu Chien<sup>1,2</sup>

<sup>1</sup>Department of Bioengineering and the Whitaker Institute of Biomedical Engineering, <sup>2</sup>Department of Medicine, <sup>3</sup>Howard Hughes Medical Institute and Departments of Pharmacology and Chemistry and Biochemistry, University of California at San Diego, La Jolla, California 92093, USA  
<sup>4</sup>Department of Biomedical Engineering, <sup>5</sup>Beckman Laser Institute, University of California at Irvine, Irvine, California 92697, USA

The mechanical environment crucially influences many cell functions<sup>1</sup>. However, it remains largely mysterious how mechanical stimuli are transmitted into biochemical signals. Src is known to regulate the integrin–cytoskeleton interaction<sup>2</sup>, which is essential for the transduction of mechanical stimuli<sup>3–5</sup>. Using fluorescent resonance energy transfer (FRET), here we develop a genetically encoded Src reporter that enables the imaging and quantification of spatio-temporal activation of Src in live cells. We introduced a local mechanical stimulation to human umbilical vein endothelial cells (HUVECs) by applying laser-tweezer traction on fibronectin-coated beads adhering to the cells. Using the Src reporter, we observed a rapid distal Src activation and a slower directional wave propagation of Src activation along the plasma membrane. This wave propagated away from the stimulation site with a speed (mean  $\pm$  s.e.m.) of  $18.1 \pm 1.7 \text{ nm s}^{-1}$ . This force-induced directional and long-range activation of Src was abolished by the disruption of actin filaments or microtubules. Our reporter has thus made it possible to monitor mechanotransduction in live cells with spatio-temporal characterization. We find that the transmission of mechanically induced Src activation is a dynamic process that directs signals via the cytoskeleton to spatial destinations.

Mechanical stimuli activate integrins and the cytoskeleton to regulate cellular functions such as movement and adhesion<sup>6</sup>. When activated, integrins associate with Src via its SH3 domain, thus unmasking the Src kinase domain and activating Src<sup>7</sup>. Src can regulate integrin–cytoskeleton interaction<sup>2</sup>, and cause dissolution of actin stress fibres and the release of mechanical tensile stress<sup>8,9</sup>.

We previously developed a FRET-based Src indicator<sup>10</sup>, but that reporter also responded to Abl, Lck and epidermal growth factor receptor (EGFR). Furthermore, mutation of the Tyr within the substrate sequence to Phe did not eliminate the FRET response, which cast doubt on the mechanism for the FRET response. We therefore sought an indicator with higher specificity and a better-defined response mechanism. A Src substrate peptide (WMEDYDYVHLQG, derived from a primary *in vivo* c-Src substrate-molecule p130cas<sup>11,12</sup>) was designed to replace the original substrate (EIYGEF, identified by *in vitro* library screening<sup>13</sup>) and to provide sufficient space for Src to gain access<sup>14</sup> (Fig. 1a). The proximity of the N and C terminals of the SH2 domain, revealed by its crystal structure<sup>15</sup>, should allow the juxtaposition of cyan and yellow fluorescent proteins (CFP and YFP) to yield a high FRET. On Src phosphorylation, the substrate peptide can bind to the phosphopeptide-binding pocket of the SH2 domain and separate YFP from CFP, thus decreasing the FRET (Fig. 1b). Phosphorylation of the purified reporter by Src *in vitro* enhanced CFP emission at the expense of YFP emission (Fig. 1c) and increased the cyan-to-yellow emission ratio by 25%, indicating a Src-induced loss of FRET. The specificity was very much better than for the previous Src indicator. The emission ratio changed by <2% for other kinases (Yes, FAK, EGFR, Abl, Jak2 or Ser/Thr kinase ERK1) and changed moderately

(~10%) only for Fyn, a close relative of Src (Fig. 1d). The Src-induced loss of FRET is consistent with intramolecular complexation of the phosphorylated substrate with the SH2 domain and the consequent disruption of the close apposition of the CFP and YFP domains (Fig. 1b).

In HeLa cells transfected with the Src reporter, epidermal growth factor (EGF) induced a 25–35% emission ratio change (Fig. 2a; Supplementary Movie 1). Introduction of the reporter did not affect the ERK activity with or without EGF stimulation (data not shown), suggesting that the reporter need not perturb endogenous cellular signalling. Mutations of either or both of the putative Src phosphorylation sites (Tyr 662 and 664) to Phe in the substrate peptide (Fig. 1a) prevented the FRET response to EGF in HeLa cells (Fig. 2b). Mutation of Arg 175 to Val (Fig. 1a), eliminating SH2 domain binding to phosphorylated peptides<sup>15</sup>, also abrogated the EGF-induced FRET response. These results validate the phosphorylation-induced intramolecular (intra-reporter) interaction between the SH2 domain and substrate peptide as the mechanism for the FRET response. Immunoblotting revealed that EGF-induced tyrosine phosphorylation is abolished only by mutating both Tyr 662 and 664, but not either site alone (Fig. 2c), unlike the blockade of the FRET response by single mutations (Fig. 2b). Thus, the SH2 binding requires not only the phosphorylation of one of the two Tyr residues but also the integrity of the other Tyr in the substrate, consistent with the notion that the neighbouring amino acids of the phosphorylated site are important for SH2 binding<sup>16</sup>. Disruption of the SH2 domain by R175V mutation also blocked the EGF-induced tyrosine phosphorylation of the Src reporter (Fig. 2c), suggesting that the SH2 domain of the reporter may assist in its association with activated Src to facilitate the phosphorylation process.

The EGF-induced FRET response in HeLa cells was reversed by PP1, a selective inhibitor of Src family tyrosine kinases, and was markedly reduced after pretreatment with PP1 (Fig. 2d). The

normal platelet-derived growth factor (PDGF)-induced FRET response of the Src reporter was abolished in Src/Yes/Fyn triple-knockout (SYF<sup>-/-</sup>) mouse embryonic fibroblasts (MEF) (Fig. 2e). Reconstitution of these SYF<sup>-/-</sup> cells with c-Src, but not c-Fyn, restored the FRET response. Reconstitution with c-Yes caused only a weak FRET response of the Src reporter. The small and delayed FRET response observed in the kinase-dead c-Src (Src\_KD) group may be attributed to the residual activity of Src\_KD. These results demonstrated the specificity of the Src reporter toward Src in mammalian cells.

CFP and YFP can form anti-parallel dimers<sup>17</sup>. To eliminate the unintended FRET resulting from intermolecular (between reporters) dimerization, we introduced A206K mutations into CFP and YFP to generate monomeric CFP and YFP<sup>18</sup> (Fig. 1a). These mutations did not alter the spectral properties of the Src reporter, but they led to a better dynamic range of FRET (43 versus 25% emission ratio change) in response to Src kinase *in vitro* (compare Fig. 2f with Fig. 1c) and a greater EGF-induced FRET response in HeLa cells that was reversible by EGF washout (Fig. 2g, Supplementary Fig. 1 and Supplementary Movie 2). This monomeric reporter was used for the study of mechano-activation of Src.

Beads coated with fibronectin, which binds to integrins and hence causes coupling with the cytoskeleton<sup>19</sup>, were applied to HUVECs. Consistent with the observation of Src activation by integrin clustering<sup>7</sup>, the fibronectin-coated beads caused a local FRET response of the Src reporter around the beads (Fig. 3a and Supplementary Movie 3), reversible by PP1 (Supplementary Fig. 2 and Supplementary Movie 4). Single-beam gradient optical laser-tweezers with controlled mechanical force (300 pN) were used to pull the adhered beads. FRET responses occurred in focal-complex-like regions at the cell periphery without detectable bead displacement (Supplementary Fig. 3a and Supplementary Movie 5). Polylysine-coated beads subjected to the same mechanical force did

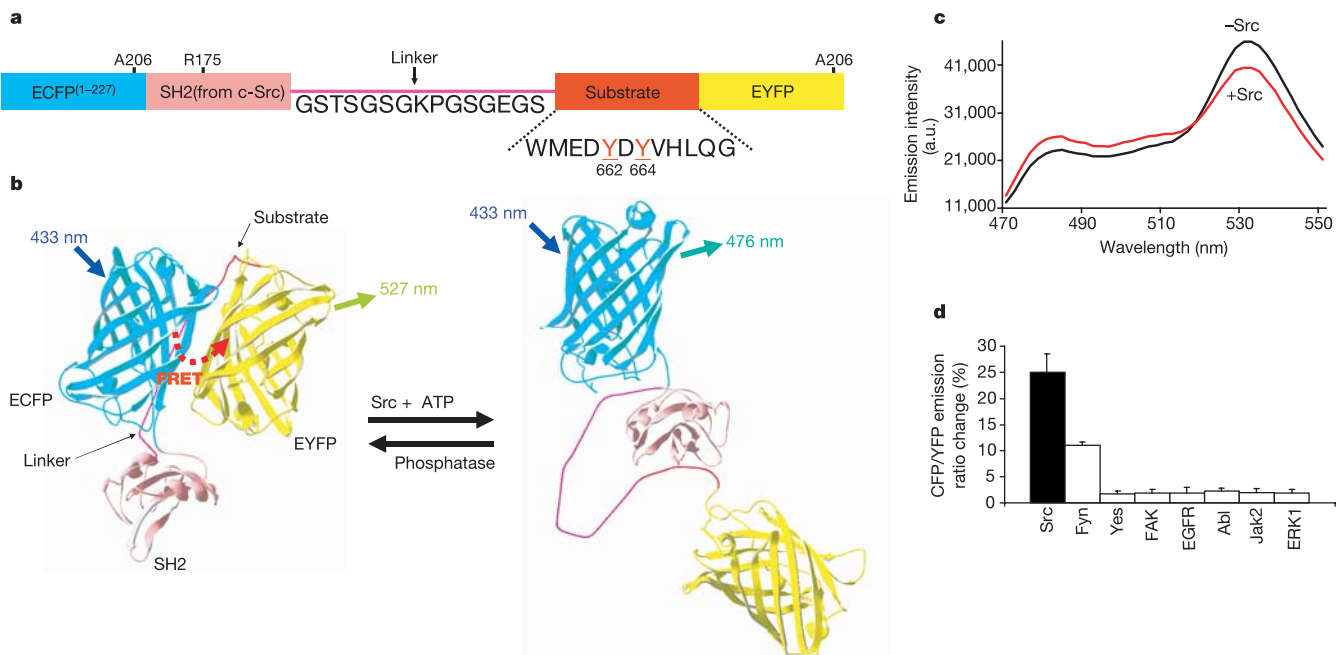


**Figure 1** The domain structure, schematic representation and *in vitro* characterizations of the Src reporter. **a**, The Src reporter is composed of CFP, the SH2 domain, a flexible linker, the Src substrate peptide and YFP (ref. 10). **b**, The cartoon illustrates the FRET effect of the Src reporter upon the actions of Src kinase or phosphatase. **c**, Emission

spectra of the Src reporter before (black) and after (red) phosphorylation by Src. **d**, *In vitro* emission ratio changes (mean  $\pm$  s.d.) of the Src reporter in response to Src and other kinases.

not induce any significant FRET response (Supplementary Fig. 3b and Supplementary Movie 6), suggesting that specific integrin–cytoskeleton coupling is needed for the mechanotransduction.

The thin lamellipodia at the cell periphery, which are important in mechanotransduction, contain only limited copies of cytosolic Src reporters. Because significant amounts of CFP/YFP molecules are required to yield enough fluorescence above the endogenous autofluorescence background<sup>20</sup>, there is a need for controlled localization of the Src reporter to enhance its effective local concentration, especially in lamellipodia. Because the translocation of Src to the plasma membrane is a prerequisite for Src activation<sup>7,21</sup>, we targeted the monomeric Src reporter to the plasma membrane with a fusion of the 16 N-terminal residues from Lyn kinase<sup>18</sup>. The EGF-induced FRET response of this membrane-targeted reporter was reversed by PP1 (Supplementary Fig. 4a and Supplementary Movie 7) and prevented by pretreatment with PP1 (Supplementary Fig. 4b and Supplementary Movie 8), indicating its specificity towards Src (Fig. 3b).

The application of pulling force via the laser tweezers on a bead coated with fibronectin, but not polylysine (Supplementary Fig. 5), on the HUVECs expressing the membrane-targeted Src reporter led to a directional FRET response, with the majority of activations

transmitted towards distal areas of the cell opposite to the force direction (Fig. 3c; Supplementary Movie 9). This transmission consisted of an immediate distal Src activation and a slower wave-propagation of Src activation followed by lamellipodia protrusions at the cell periphery (Fig. 3c). Such FRET responses were absent with inactive reporters (for Y662F/Y664F see Supplementary Fig. 6a and Supplementary Movie 10; for R175V see Supplementary Fig. 6b and Supplementary Movie 11). In experiments where the speed of the wave propagation of Src-activation away from the stimulation site can be clearly measured, it was found to be  $18.1 \pm 1.7 \text{ nm s}^{-1}$  (mean  $\pm$  s.e.m.) (Fig. 3d; Supplementary movie 12). This result indicates that a local force caused a directional and long-range transduction of Src-activation wave to spatial destinations.

We examined the roles of the cytoskeleton on this force-induced Src activation. Disruption of actin filaments with cytochalasin D or microtubules with nocodazole blocked the force-induced distal, but not local, FRET responses (Fig. 4a, b; Supplementary Movies 13, 14). Polarity analysis of Src activation, by averaging the emission ratios of 36 evenly divided angular sections of each cell with the bead position as the centre, revealed that the local pulling force caused a cytoskeleton-dependent polarized

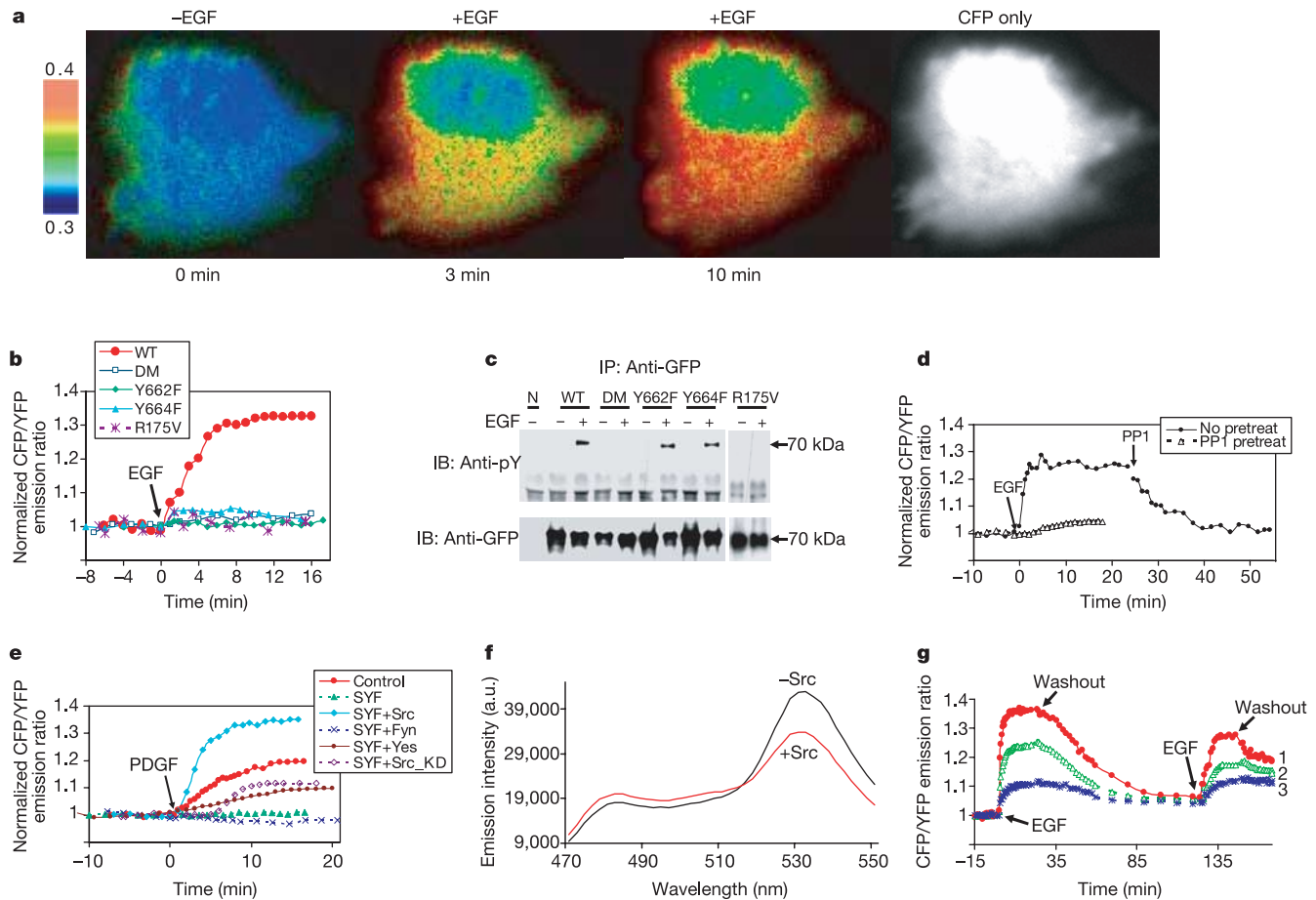


**Figure 2** Characterization of the Src reporters. **a**, The CFP/YFP emission ratio images in response to EGF (Supplementary Movie 1). **b**, Emission ratio time courses of the Src reporter and its mutants (see Methods) in response to EGF stimulation in HeLa cells. **c**, The tyrosine phosphorylation level of the various Src reporters (see Methods). 'N' represents cells without transfection. **d**, Emission ratio time courses of the Src reporter in response to EGF in HeLa cells pretreated with ('PP1 pretreat') or without ('No pretreat')

PP1. **e**, Emission ratio time courses of the Src reporter in response to PDGF in MEF and SYF cell lines (see Methods). **f**, Emission spectra of the monomeric Src reporter before (black) and after (red) *in vitro* phosphorylation by Src. **g**, Emission ratios of the monomeric Src reporter from three different subcellular regions in HeLa cells stimulated by EGF, followed sequentially by EGF washout, re-stimulation, and a second washout (Supplementary Movie 2).

FRET response pointing to the opposite direction (Fig. 4c, d). Statistical analysis further showed that the mechanical force caused a cytoskeleton-dependent increase of the number of pixels with highly activated Src distal to the force-imposed bead, indicating a long-range mechano-activation of Src (Fig. 4e; Supplementary Fig. 7).

It is unclear where mechano-induced biochemical signals are initiated and how they are transmitted in the cell. Green fluorescent protein (GFP)-tagged fluorescent markers have been used to study the displacement of cellular organelles and the formation of a focal adhesion complex induced by mechanical stimuli<sup>22–25</sup>, but these inert fluorescence markers cannot monitor the dynamic signal transduction process. Our FRET-based Src reporter enables the visualization and quantification of the mechano-activated Src with high temporal and spatial resolution in live cells. The results indicate that local mechanical stimulation triggers a directional and

long-range propagation of Src activation, for which cytoskeleton integrity is essential.

Integrin-mediated activation of Src at local sites by mechanical stimuli may induce p130cas/Dock180 association, Rac-Arp2/3 activation, cortical actin network nucleation and polymerization, and actin-ruffle extensions<sup>26,27</sup>. These Rac and actin activities in turn promote the recruitment and activation of Src at the tip of these newly assembled wave-like actin ruffles<sup>28,29</sup>, thus further inducing the *in situ* Rac activation and actin polymerization. This positively coordinated mechanism may result in a wave propagation of Src activation. The directionality of this wave propagation may be attributed to the initial local mechanical tension generated in a direction counter to the applied force. The applied force can also be mechanically transmitted quickly through tensed cytoskeleton network to distal locations and to activate Src<sup>1</sup>. This directional Src activation may release the tension<sup>21</sup> at desired destinations and

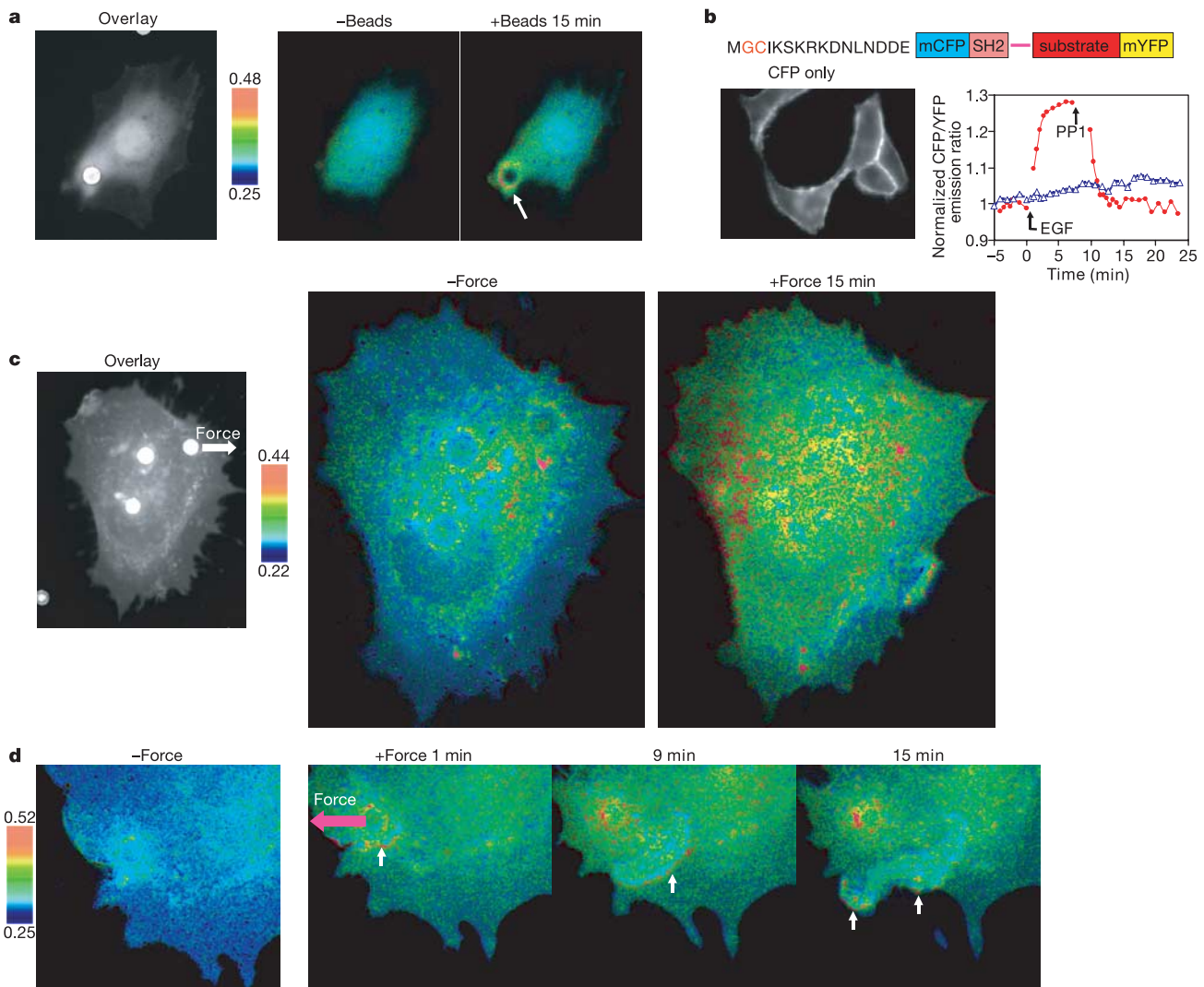


**Figure 3** Directional and long-range propagation of Src induced by mechanical force. **a**, A fibronectin-coated bead (white spot from phase contrast image overlaid on CFP cell image) induced FRET responses around the bead (Supplementary Movie 3). White arrow points to the spot with activated Src. Colour bar represents CFP/YFP emission ratio values. **b**, The schematic diagram in the upper panel shows the design strategy of membrane targeting. The CFP-only image on the left shows the effective tethering of the reporter on the plasma membrane. The EGF-induced FRET responses of the reporter is reversed by

PP1 (red line; Supplementary Movie 7) and prevented by pretreatment with PP1 (blue line; Supplementary Movie 8). **c**, Laser-tweezer traction on the bead at the upper right corner of the cell (shown on the left) caused FRET responses (Supplementary Movie 9). White arrow represents force direction. **d**, FRET responses of a cell with clear directional wave propagation away from the site of mechanical stimulation (Supplementary Movie 12).

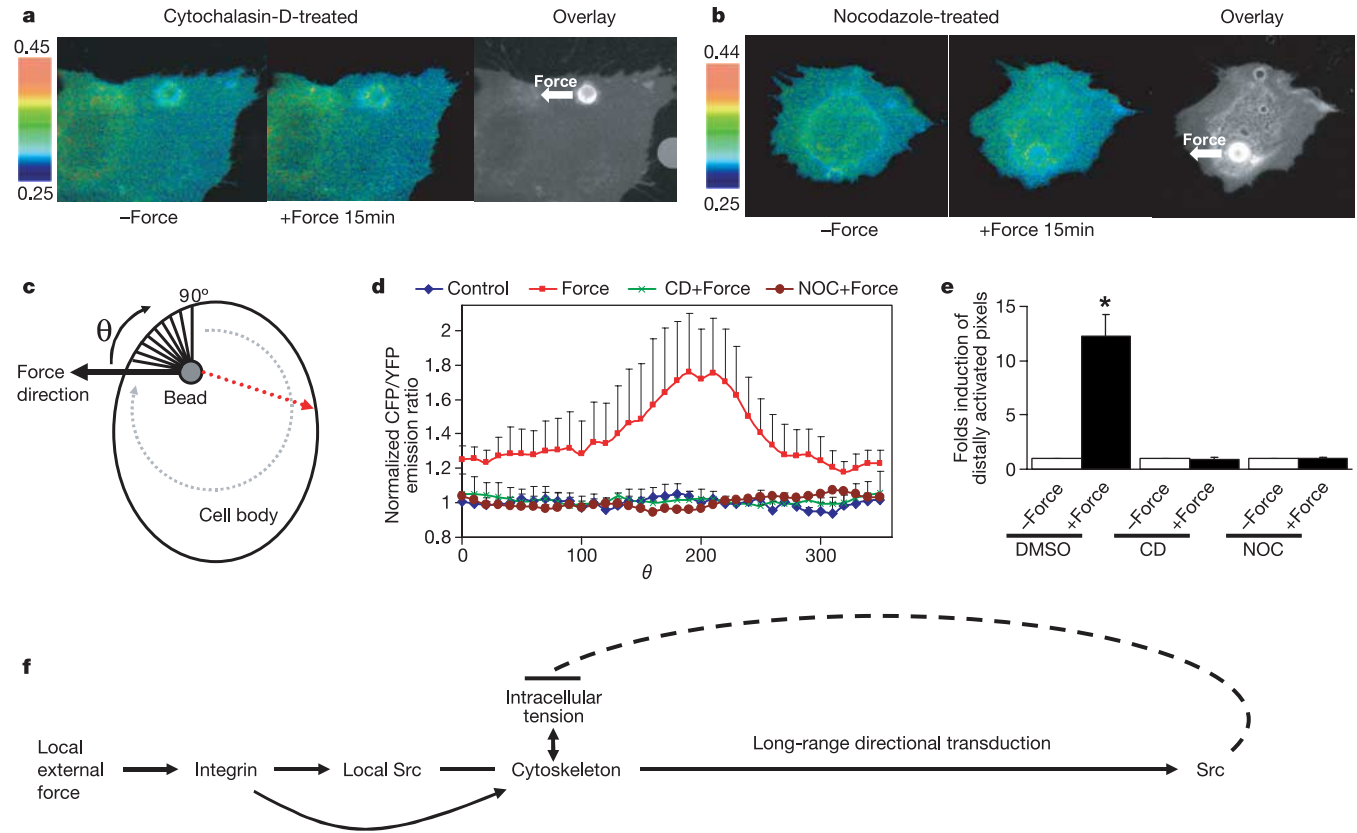


**Figure 4** Actin filaments and microtubules are essential for the polarized and long-range Src activation. Emission ratio images of HUVECs pretreated with cytochalasin D (**a**, Supplementary Movie 13) or nocodazole (**b**, Supplementary Movie 14) before and after force application. **c**, Schematic drawing of the polarity analysis strategy. **d**, Polarity analysis (mean  $\pm$  s.d.) of the force-induced FRET response. Control, no force application. CD or NOC, cytochalasin D or nocodazole treatment, respectively. **e**, HUVECs treated with

cytochalasin D, nocodazole or DMSO were subjected to mechanical force for 15 min or kept as static control. Bar graphs represent mean  $\pm$  s.d. of the force-induced fold induction of distally activated (see Methods, with 80% threshold) pixel numbers. The asterisk indicates a significant difference ( $P < 0.05$ ) before and after force application. **f**, A proposed model depicting the mechanism by which local mechanical forces induce directional and long-range Src activations.

rearrange the intracellular stress distribution, thus serving as a feedback mechanism for the cell to adapt to new mechanical environments (Fig. 4f). □

**Methods**

**Laser-tweezers**

A 1064-nm continuous-wave diode-pumped ND:YV0<sub>4</sub> laser with 5W power (Spectra-Physics) was used for the laser-tweezers experiments. The laser beam passes through a laser-beam expander, a steering mirror, and a dichroic long-pass beamsplitter to enter the microscope side port.

**Gene construction and DNA plasmids**

The gene for the Src reporter was constructed by polymerase chain reaction (PCR) amplification of the complementary DNA from the c-Src SH2 domain with a sense primer containing a *SphI* site and a reverse primer containing the gene sequence for a flexible linker, a substrate peptide derived from p130cas, and a *SacI* site. The PCR products were fused together with an N-terminal enhanced CFP and a C-terminal citrine (a version of enhanced YFP)<sup>10</sup>, as shown in Fig. 1a. Mutations of Y662/664F, Y662F, Y664F, R175V and A206K were conducted with the QuickChange method (Stratagene). Constructs were cloned into pRSET<sub>B</sub> (Invitrogen) using *Bam*HI/*Eco*RI for bacterial expression and into pcDNA3 (Invitrogen) behind a Kozak sequence using *Hind*III/*Eco*RI for mammalian cell expression. The membrane-targeted CFP was constructed by PCR amplification of the monomeric CFP with a sense primer containing the codes for 16 N-terminal amino acids from Lyn kinase<sup>18</sup> to produce a membrane-targeted Src reporter.

The various Src reporters and their mutants used in Figs 2b and c are abbreviated as: WT, the Src reporter (wild type); DM, Y662F and Y664F double mutations in the designed substrate peptide; Y662F or Y664F, the Y662F or Y644F single mutation in the substrate peptide, respectively; and R175V, the R175V mutation in the binding pocket of the SH2 domain.

**Cell lines**

The various mouse embryonic fibroblasts (MEFs) and knockout cell lines used for specificity studies in Fig. 2e are: wild type (control), Src/Yes/Fyn triple-knockout (SYF), SYF reconstituted with c-Src (SYF+Src), c-Fyn (SYF+Fyn), c-Yes (SYF+Yes), or K295R kinase-dead c-Src (SYF+Src\_KD).

**Microscopy and image acquisition**

The HeLa or MEF cells expressing the desired exogenous proteins were starved with 0.5% FBS for 36–48 h before being subjected to EGF (50 ng ml<sup>-1</sup>) or PDGF (10 ng ml<sup>-1</sup>) stimulation. During imaging, the cells were maintained in Hanks' balanced salt solution (HBSS) with 20 mM HEPES (pH 7.4) and 2 g l<sup>-1</sup> D-glucose at 25 °C. Images were collected by using MetaFluor 6.0 software (Universal Imaging) with a 440DF20 excitation filter, a 455DRLP dichroic mirror, and two emission filters controlled by a filter changer (480DF30 for CFP and 535DF25 for YFP).

To image the mechanical-force-induced Src activation, HUVECs were first starved with 0.5% FBS for 24 h and then kept in CO<sub>2</sub>-independent medium without serum (Gibco BRL) at 37 °C in a thermostatic chamber. A Zeiss axiovert inverted microscope equipped with a 440DF20 excitation filter and a 455DRLP dichroic mirror was integrated with the laser-tweezers. CFP and YFP emission images were acquired simultaneously with an ORCA ER CCD camera (Hamamatsu) through a Dual-View module (Optical-Insights). The CFP and YFP images were aligned pixel-by-pixel with our customized Matlab program by maximizing the normalized cross-correlation coefficient of CFP and YFP fluorescence intensity images:

$$\text{corr} = \frac{\sum_i \sum_j (C_{ij} - \bar{C})(Y_{ij} - \bar{Y})}{\sqrt{\left(\sum_i \sum_j (C_{ij} - \bar{C})^2\right) \left(\sum_i \sum_j (Y_{ij} - \bar{Y})^2\right)}}$$

Where  $C_{ij}$  and  $Y_{ij}$  are the intensity values at pixels ( $i, j$ ) of the CFP and YFP images, and  $\bar{C}$  and  $\bar{Y}$  are the mean intensity values of the CFP and YFP images. The ratio images of aligned CFP/YFP were computed and created by the MetaFluor software to represent the FRET efficiency.

Image analysis

By taking the derivative of  $\sigma_B^2(\kappa)$  in Otsu's method<sup>30</sup> and calculating its first local minimum, a non-parametric method was developed to calculate the intensity threshold to differentiate the edges of HUVECs from the background in CFP or YFP fluorescence intensity images. The intensity threshold was used to generate a binary mask image with values outside the cell set at zero to select the pixels located within the cell body in the CFP/YFP emission ratio images. For polarity analysis, a customized Matlab program was used to evenly divide a HUVEC into 36 angular sections with the bead position as the centre and the force direction as the zero degree axes for  $\theta$ , as illustrated in Fig. 4c. For statistical analysis of long-range activation of Src, a pixel located within a cell at a given time is defined as 'distally activated' when: (1) its emission ratio value is above a certain percentage (98%, 90%, 80% and 50% were used as the thresholds) of pixel population in the same cell after 15 min of force stimulation, and (2) the distance between the pixel and the centre of the force-imposed bead is larger than half of the virtual radius of the cell, as shown in the following formula:

$$\sqrt{(x-x_0)^2+(y-y_0)^2} > \frac{R}{2} = \frac{1}{2} \sqrt{\frac{A}{\pi}}$$

where  $x, y$  are the coordinates of any given pixel within the cell body,  $x_0, y_0$  are the coordinates of the force-imposed bead centre,  $R$  is the virtual radius for the cell, and  $A$  is the area of the cell.

Received 2 November 2004; accepted 11 February 2005; doi:10.1038/nature03469.

1. Ingber, D. E. Tensegrity. II. How structural networks influence cellular information processing networks. *J. Cell. Sci.* **116**, 1397–1408 (2003).
2. Felsenfeld, D. P., Schwartzberg, P. L., Venegas, A., Tse, R. & Sheetz, M. P. Selective regulation of integrin–cytoskeleton interactions by the tyrosine kinase Src. *Nature Cell Biol.* **1**, 200–206 (1999).
3. Critchley, D. R. Focal adhesions—the cytoskeletal connection. *Curr. Opin. Cell Biol.* **12**, 133–139 (2000).
4. Chicurel, M. E., Singer, R. H., Meyer, C. J. & Ingber, D. E. Integrin binding and mechanical tension induce movement of mRNA and ribosomes to focal adhesions. *Nature* **392**, 730–733 (1998).
5. Jiang, G., Giannone, G., Critchley, D. R., Fukumoto, E. & Sheetz, M. P. Two-piconewton slip bond between fibronectin and the cytoskeleton depends on talin. *Nature* **424**, 334–337 (2003).
6. Alenghat, F. J. & Ingber, D. E. Mechanotransduction: all signals point to cytoskeleton, matrix, and integrins. *Sci. STKE* **2002**, E6 (2002).
7. Arias-Salgado, E. G. et al. Src kinase activation by direct interaction with the integrin beta cytoplasmic domain. *Proc. Natl Acad. Sci. USA* **100**, 13298–13302 (2003).
8. Fincham, V. J., Brunton, V. G. & Frame, M. C. The SH3 domain directs actin-myosin-dependent targeting of v-Src to focal adhesions via phosphatidylinositol 3-kinase. *Mol. Cell Biol.* **20**, 6518–6536 (2000).
9. Kaplan, G. et al. Identification of a surface glycoprotein on African green monkey kidney cells as a receptor for hepatitis A virus. *EMBO J.* **15**, 4282–4296 (1996).
10. Ting, A. Y., Kain, K. H., Klemke, R. L. & Tsien, R. Y. Genetically encoded fluorescent reporters of protein tyrosine kinase activities in living cells. *Proc. Natl Acad. Sci. USA* **98**, 15003–15008 (2001).
11. Hamasaki, K. et al. Src kinase plays an essential role in integrin-mediated tyrosine phosphorylation of Crk-associated substrate p130Cas. *Biochem. Biophys. Res. Commun.* **222**, 338–343 (1996).
12. Vuori, K., Hirai, H., Aizawa, S. & Ruoslahti, E. Introduction of p130Cas signaling complex formation upon integrin-mediated cell adhesion: a role for Src family kinases. *Mol. Cell Biol.* **16**, 2606–2613 (1996).
13. Songyang, Z. et al. Catalytic specificity of protein-tyrosine kinases is critical for selective signalling. *Nature* **373**, 536–539 (1995).
14. Yang, E., Liu, Y., Bixby, S. D., Friedman, J. D. & Shokat, K. M. Highly efficient green fluorescent protein-based kinase substrates. *Anal. Biochem.* **266**, 167–173 (1999).

15. Waksman, G. et al. Crystal structure of the phosphotyrosine recognition domain SH2 of v-src complexed with tyrosine-phosphorylated peptides. *Nature* **358**, 646–653 (1992).
16. Bradshaw, J. M. & Waksman, G. Calorimetric examination of high-affinity Src SH2 domain-tyrosyl phosphopeptide binding: dissection of the phosphopeptide sequence specificity and coupling energetics. *Biochemistry* **38**, 5147–5154 (1999).
17. Yang, F., Moss, L. G. & Phillips, G. N. Jr The molecular structure of green fluorescent protein. *Nature Biotechnol.* **14**, 1246–1251 (1996).
18. Zacharias, D. A., Violin, J. D., Newton, A. C. & Tsien, R. Y. Partitioning of lipid-modified monomeric GFPs into membrane microdomains of live cells. *Science* **296**, 913–916 (2002).
19. Miyamoto, S. et al. Integrin function: molecular hierarchies of cytoskeletal and signaling molecules. *J. Cell Biol.* **131**, 791–805 (1995).
20. Tsien, R. Y. The green fluorescent protein. *Annu. Rev. Biochem.* **67**, 509–544 (1998).
21. Thomas, S. M. & Brugge, J. S. Cellular functions regulated by Src family kinases. *Annu. Rev. Cell Dev. Biol.* **13**, 513–609 (1997).
22. Heidermann, S. R., Kaech, S., Buxbaum, R. E. & Matus, A. Direct observations of the mechanical behaviors of the cytoskeleton in living fibroblasts. *J. Cell Biol.* **145**, 109–122 (1999).
23. Hu, S. et al. Intracellular stress tomography reveals stress focusing and structural anisotropy in cytoskeleton of living cells. *Am. J. Physiol. Cell Physiol.* **285**, C1082–C1090 (2003).
24. Mack, P. J., Kaazempur-Mofrad, M. R., Karcher, H., Lee, R. T. & Kamm, R. D. Force-induced focal adhesion translocation: effects of force amplitude and frequency. *Am. J. Physiol. Cell Physiol.* **287**, C954–C962 (2004).
25. Riveline, D. et al. Focal contacts as mechanosensors: externally applied local mechanical force induces growth of focal contacts by an mDia1-dependent and ROCK-independent mechanism. *J. Cell Biol.* **153**, 1175–1186 (2001).
26. Brugnera, E. et al. Unconventional Rac-GEF activity is mediated through the Dock180-ELMO complex. *Nature Cell Biol.* **4**, 574–582 (2002).
27. Miki, H., Suetsugu, S. & Takenawa, T. WAVE, a novel WASP-family protein involved in actin reorganization induced by Rac. *EMBO J.* **17**, 6932–6941 (1998).
28. Sandilands, E. et al. RhoB and actin polymerization coordinate Src activation with endosome-mediated delivery to the membrane. *Dev. Cell* **7**, 855–869 (2004).
29. Timpson, P., Jones, G. E., Frame, M. C. & Brunton, V. G. Coordination of cell polarization and migration by the Rho family GTPases requires Src tyrosine kinase activity. *Curr. Biol.* **11**, 1836–1846 (2001).
30. Otsu, N. Threshold selection method from Gray-level histograms. *IEEE Trans. Syst. Man Cybern.* **9**, 62–66 (1979).

Supplementary Information accompanies the paper on [www.nature.com/nature](http://www.nature.com/nature).

**Acknowledgements** We thank J. Zhang and A. Y. Ting for their assistance and advice; J.-L. Guan, D. C. Flynn and J. Cooper for providing FAK protein, MEF cells, c-Yes plasmid and SYF cell lines. We also thank B. N. G. Giepmans and C. Hauser for their comments on the paper, and Q. Xiong for technical support. This work was supported by the National Institutes of Health (S.C., R.Y.T. and M.W.B.), the Howard Hughes Medical Institute (R.Y.T.), the Airforce Office of Scientific Research (M.W.B.), the Arnold and Mabel Beckman Foundation (E.L.B.) and the Alliance for Cellular Signaling Grant (R.Y.T., S.C. and Y.W.).

**Competing interests statement** The authors declare that they have no competing financial interests.

**Correspondence** and requests for materials should be addressed to S.C. (schien@bioeng.ucsd.edu). The sequence reported in this paper has been deposited in the GenBank database (accession number AY862145).